Organic Electronics 9 (2008) 747–752

Contents lists available at ScienceDirect

Organic Electronics

journal homepage: www.elsevier.com/locate/orgel

Organic photovoltaic cells with high open circuit voltages based on pentacene derivatives

Leonidas C. Palilis [a,1], Paul A. Lane [a,*], Gary P. Kushto [a], Balaji Purushothaman [b], John E. Anthony [b], Zakya H. Kafafi [a,2]

[a] US Naval Research Laboratory, 4555 Overlook Avenue SW, Washington, DC 20375-5611, United States
[b] Department of Chemistry, University of Kentucky, Lexington, KY 40506-0055, United States

ARTICLE INFO

Article history:
Received 4 March 2008
Received in revised form 8 May 2008
Accepted 10 May 2008
Available online 16 June 2008

PACS:
73.50.Gr
78.40.Me
84.60.Jt

Keywords:
Pentacene
Organic photovoltaics
Fullerene
Morphology

ABSTRACT

Heterojunction organic photovoltaic devices were fabricated using C_{60} as the electron acceptor and several pentacene derivatives with triisopropylsilylethynyl functional groups as the electron donor. The open circuit voltage (V_{oc}) of functionalized pentacene-based cells is significantly higher (0.57–0.90 V) than for cells based on unsubstituted pentacene (0.24 V), due to the higher oxidation potentials of these pentacene derivatives. The performance of pentacene derivative cells is limited by lower current densities than the reference pentacene/C_{60} cell. The absorption spectra of films and solutions of pentacene derivatives closely resemble one another, leading us to conclude that these films are amorphous in nature. Weak intermolecular coupling in the derivative films results in lower charge mobility and shorter exciton diffusion lengths relative to pentacene.

Published by Elsevier B.V.

1. Introduction

Organic photovoltaics based on molecular semiconductors have attracted significant scientific and commercial interest due to their potential use for low cost flexible solar cells. The primary device architecture used in molecular solar cells is a multi-layer structure where charge photogeneration occurs at interfaces between electron donor and acceptor molecules [1,2]. Materials employed in solar cells should ideally have strong absorption overlapping the solar spectrum, efficient exciton diffusion to the interface and high charge carrier mobility. Fused acenes comprise a class of materials that have recently been used in organic photovoltaics. Tetracene [3,4] and pentacene [5–9] have been used in cells with efficiencies of ~2% under simulated solar illumination. Pentacene is a particularly promising material due to its strong absorption in the visible part of the solar spectrum [10] and high field-effect mobility, as high as 3 $cm^2/V\,s$ in thin film transistors [11]. The performance of pentacene-based solar cells has been limited by their relatively low open circuit voltage (V_{oc}), a direct consequence of the small offset between the highest occupied molecular orbital (HOMO) of pentacene (4.9 eV) [12] and the lowest unoccupied molecular orbital (LUMO) of C_{60}.

Recently, Anthony and co-workers modified the chemical structure of pentacene in order to change its optical and electronic properties [13–15]. They sought to increase the

* Corresponding author.
E-mail addresses: lpalil@imel.demokritos.gr (L.C. Palilis), paul.lane@nrl.navy.mil (P.A. Lane).
[1] Present address: Institute of Microelectronics, National Center for Scientific Research "Demokritos", P.O. Box 60228, 15310 Aghia Paraskevi, Attiki, Greece.
[2] Present address: National Science Foundation, 4201 Wilson Boulevard, Suite 1065 North, Arlington, VA 22230, United States.

1566-1199/$ - see front matter Published by Elsevier B.V.
doi:10.1016/j.orgel.2008.05.015

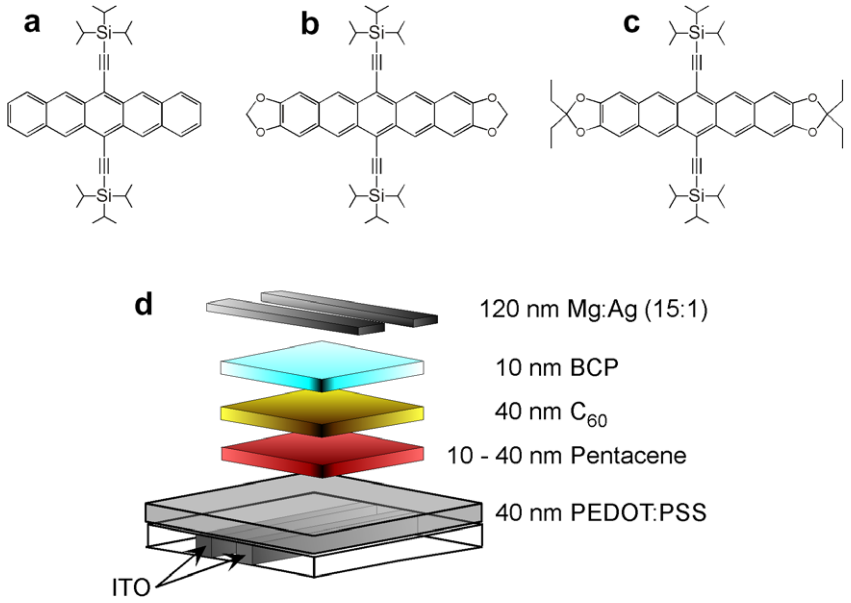

Fig. 1. Chemical structures of (a) TIPS, (b) TP-5, (c) EtTP-5, and (d) schematic diagram of the photovoltaic cells.

intermolecular π-orbital overlap in the crystalline form in order to improve carrier mobility, lower the energy of the HOMOs in order to increase the open circuit voltage of solar cells, and modify the absorption spectrum in order to harvest more solar light. To this end, triisopropylsilylethynyl functional groups were added at the 6,13-positions of pentacene and 1,3-dioxolane moieties were fused to the terminal benzenoid rings of the pentacene molecule. The chemical structures of (a) 6,13-bis(triisopropylsilylethynyl)-pentacene (TIPS), (b) 6,14-bis(tri-isopropylsilylethynyl)-1,3,9,11-tetraoxacyclopenta[*b*,*m*]pentacene (TP-5) and (c) 2,2,10,10-tetraethyl-6,14-bis(tri-isopropylsilylethynyl)-1,3,9,11-tetraoxacyclopenta[*b*,*m*]pentacene (EtTP-5) are shown in Fig. 1. These pentacene derivatives have been used as fluorescent dopant molecules in organic light-emitting diodes [16–18]. More recently, Lloyd et al. investigated multi-layer, solution-processed solar cells using TIPS as an electron donor [19]. In this study, we report on the fabrication and characterization of organic solar cells using this series of pentacene derivatives as electron donors. Our approach differs from that of Lloyd et al. in that all layers in our cells are formed by vacuum sublimation. We obtain significantly higher V_{oc} from the derivative-based cells than for reference pentacene-based cells and correlate this increase with their higher oxidation potentials. Despite the lower short circuit photocurrent (J_{sc}) of the derivative-based cells, a power conversion efficiency of 0.74% was obtained from a dioxalane-based pentacene with high V_{oc}, comparable to that of a reference cell (0.82%).

2. Experimental

The synthesis of TIPS and TP-5 was previously reported [13]. EtTP-5 was prepared by the addition of triisopropylsilyl acetylide to the corresponding quinone [20], followed by deoxygenation with aqueous stannous chloride/10% H_2SO_4. C_{60} was purchased from SES (Houston, TX) while both pentacene and 2,9-dimethyl-4,7-diphenyl-1,10-phenanthroline were purchased from Aldrich (Milwaukee, WI). All materials were purified twice via vacuum train sublimation prior to use. The oxidation potential measurements were performed by cyclic voltammetry in dichloromethane solution vs ferrocene as the internal standard.

Fig. 1d shows the multi-layer device architecture we employed for organic photovoltaics. Indium tin oxide (ITO) coated by poly(3,4-ethylenedioxythiophene):poly(styrenesulfonate) (PEDOT:PSS) was used as the anode. The ~40 nm thick PEDOT:PSS layer was spin-cast from a pre-filtered aqueous solution onto ozone-cleaned ITO-coated glass substrates (ITO thickness = 100 nm, sheet resistance = 15 Ω/square) and then annealed in air at 130 °C for 10 min. Pentacene or one of its derivatives acted as the electron donor and hole transport material and C_{60} as the electron acceptor and electron transport material. A 10 nm thick layer of 2,9-dimethyl-4,7-diphenyl-1,10-phenanthroline, also known as bathocuproine (BCP), was deposited on top of the C_{60} layer to prevent exciton quenching at the C_{60}/cathode interface. The organic layers were sequentially deposited onto the ITO/PEDOT:PSS substrates by vacuum thermal evaporation under a background pressure of $<10^{-6}$ Torr at a rate of ~0.5–1 Å s^{-1}. The thickness of the pentacene layer was varied between approximately 10 and 40 nm while that of C_{60} was fixed at 40 nm. Finally, a ~130 nm thick metal Mg:Ag cathode (10:1 by weight) was co-deposited through a shadow mask from separate evaporation sources. The active device area was 4 mm^2. Optical absorption spectra were measured with an HP 8423 UV–vis spectrophotometer.

The photovoltaic devices were spectroscopically and electrically characterized in an inert atmosphere, N_2 glove

box (O_2 and H_2O < 1 ppm) at room temperature, immediately following their fabrication. The current–voltage characteristics, both in the dark and under simulated AM 1.5 solar illumination at 100 mW/cm^2 (1 sun), were measured by a Keithley multimeter. The series resistance was calculated by a linear regression to the dark JV curve above 1 V. A good fit to the Schockley equation, modified for series and shunt resistance, could not be obtained for these devices. The solar light intensity was measured with a calibrated silicon photodiode and varied using neutral density filters. The spectral response of the cells was characterized by incident photon-to-current efficiency (IPCE) measurements.

3. Results and discussion

Fig. 2 shows the extinction spectra of (a) thin films and (b) dilute toluene solutions of the pentacene derivatives; the thin film extinction spectrum of pentacene is shown for comparison. TIPS has a peak at $\lambda \approx 650$ nm with an extinction coefficient close to 20,000 cm^{-1} and vibronic side bands at 554 and 602 nm. The extinction spectra of both TP-5 and EtTP-5 are similar to that of TIPS in the red and contain an intense, sharp peak in the blue; $\alpha = 74{,}000$ cm^{-1} at $\lambda = 470$ nm for TP-5 and $\alpha = 62{,}000$ cm^{-1} at $\lambda = 458$ nm for EtTP-5. There is a similar, but much weaker absorption feature in the blue for TIPS ($\alpha = 9700$ cm^{-1} at $\lambda = 442$ nm). The oscillator strength of this transition is dramatically affected by the dioxolane moiety. By comparison, the pentacene absorption spectrum is red-shifted from that of the derivatives and is much stronger. The significant red-shift of the pentacene film absorption compared to its solution spectrum has been proposed to be a direct result of strong intermolecular interactions [5]. This coupling results in increased absorption in the red portion of the solar spectrum, which enhances photocurrent generation. In contrast, the thin film and solution spectra of the pentacene derivatives are remarkably similar, suggesting that solid state interactions are relatively weak in these films. The solid state spectra are slightly broader than the solution spectra and only the absorption spectrum of TP-5 has a limited red-shift (~20 nm) from solution to thin film. Ostroverkhova et al. [21] studied the morphology and photoconductivity of TIPS films prepared under different conditions and showed that it is possible to obtain larger crystalline domains, particularly by crystallization from solution. Such films exhibit significantly red-shifted absorption, with an absorption edge at ~750 nm. Films prepared by sublimation under vacuum onto a heated substrate also showed evidence of crystallization. The limited red-shift and absence of new features strongly suggest that the films sublimed onto an unheated substrate are essentially amorphous, though the presence of some crystallinity cannot be completely ruled out.

Fig. 3 shows the dark current density–voltage (J–V) characteristics for the various photovoltaic cells with a 40 nm thick layer of pentacene or one of its derivatives. The pentacene derivative-based cells have significantly higher series resistance (R_s) than the pentacene-based cell. Cells based on pentacene exhibited a low R_s of 4.0 Ω cm^2 compared to 21.7 Ω cm^2 for TIPS, 29.8 Ω cm^2 for TP-5 and 26.2 Ω cm^2 for EtTP-5. The lower current density of devices made with pentacene derivatives vis-à-vis pentacene re-

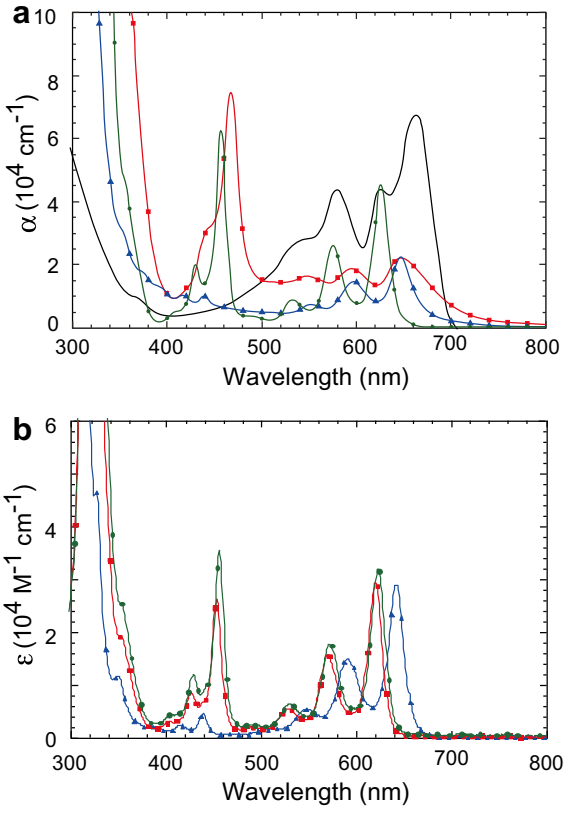

Fig. 2. (a) Thin-film extinction spectra of the pentacene derivatives TIPS (green, circles), TP-5 (red, squares), and EtTP-5 (blue, triangles). The extinction spectra of pentacene is shown for comparison (black line). (b) Solution extinction spectra of TIPS (green, circles), TP-5 (red, squares), and EtTP-5 (blue, triangles). (For interpretation of the references to colour in this figure legend, the reader is referred to the web version of this article.)

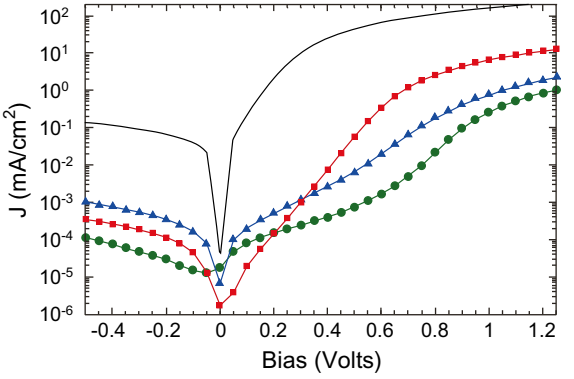

Fig. 3. Dark current density–voltage characteristics for the pentacene/C_{60} (black line) and derivative/C_{60} photovoltaic cells [TIPS (green, circles), TP-5 (red, squares), and EtTP-5 (blue, triangles)]. (For interpretation of the references to colour in this figure legend, the reader is referred to the web version of this article.)

flects the relative hole mobility in these films. The room temperature hole mobility of pentacene exceeds 1 cm^2/V s, [11], whereas Park et al. [22] measured a field-effect hole mobility of 0.02 cm^2/V s for TIPS sublimed onto a substrate at room temperature. Higher field-effect mobility from TIPS has been observed when grown from solution onto a functionalized substrate [23], although this structure differs significantly from that of a photovoltaic cell. More recently, transient THz absorption studies by Ostroverkhova et al. have also shown that the charge carrier mobility of a crystalline film of TIPS can be as high as one-third that of pentacene [21]. The much lower current densities obtained here are in agreement with the conclusion drawn from the absorption spectra – pentacene derivative films prepared by sublimation onto an unheated substrate have weak intermolecular coupling.

Fig. 4 shows the *J–V* characteristics of the various pentacene-based devices under AM1.5 illumination; Table 1 summarizes their performance. The power conversion efficiency η and the fill factor (*ff*) of the cells were calculated using

$$\eta = J_{sc} V_{oc} ff / P_0 \quad (1)$$

where J_{sc} is the short circuit current density, V_{oc} is the open circuit voltage, *ff* is the fill factor and P_0 is the incident light intensity. The fill factor is defined as the ratio between the maximum output power (P_{max}) and the product of J_{sc} and V_{oc}. The pentacene device shows good performance with V_{oc} = 0.24 V, J_{sc} = 7.6 mA/cm^2, *ff* = 0.46, and η = 0.82%. The small V_{oc}, almost half that of the more commonly reported copper phthalocyanine (CuPc)/C_{60} cell (~0.45 V) [2], reflects the lower ionization potential of pentacene (4.9 eV) [12] compared to CuPc (5.1 eV) [24]. The efficiency of the pentacene/C_{60} cell is comparable to that of similar device architectures, though the open circuit voltage is slightly lower than that reported by Mayer et al. (0.30 V) [5] and Yoo et al. (0.36 V) [6]. These variations arise from slightly different structures and fabrication conditions, particularly

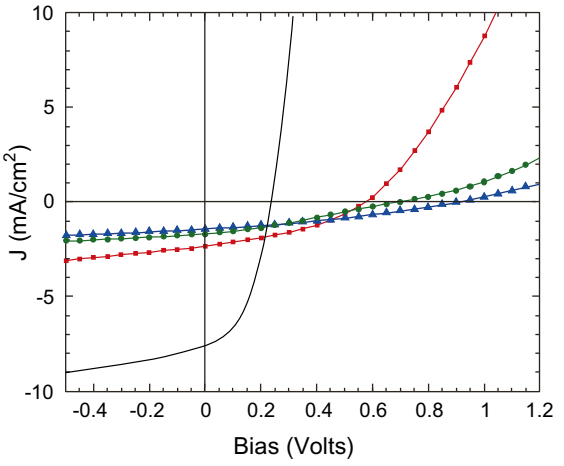

Fig. 4. Illuminated *J–V* characteristics (AM1.5, 100 mW/cm^2) for the pentacene/C_{60} (black line) and derivative/C_{60} photovoltaic cells [TIPS (green, circles), TP-5 (red, squares), and EtTP-5 (blue, triangles)]. (For interpretation of the references to colour in this figure legend, the reader is referred to the web version of this article.)

Table 1
Photovoltaic parameters of our solar cells obtained in the dark (Fig. 3) and under AM1.5 (100 mW/cm^2) solar illumination (Fig. 4)

Electron donor	E_{ox} (V)	V_{oc} (V)	J_{sc} (mA/cm^2)	*ff*	η (%)
Pentacene	0.100	0.24	7.59	0.46	0.82
TP-5	0.217	0.57	2.32	0.37	0.50
EtTP-5	0.180	0.69	1.68	0.29	0.34
TIPS	0.390	0.90	1.42	0.33	0.42

The layer thicknesses are 40 nm for the electron donor, 40 nm for C_{60}, and 10 nm for BCP. The oxidation potential data for the pentacene derivatives are listed for comparison.

the use of a different cathode, Mg:Ag in our case and either aluminum [6] or cesium fluoride capped by aluminum [5] in other studies. In comparison, the cells based on the pentacene derivatives showed a lower performance in terms of the overall cell efficiency being equal to 0.34% for EtTP-5, 0.42% for TIPS, and 0.50% for TP-5. Lloyd et al. achieved an efficiency of 0.52% from a cell using solution-processed TIPS [19], comparable to what we report here. The lower efficiency of cells based on pentacene derivatives is mainly due to the lower J_{sc}, and is also affected by the lower fill factor, owing to the larger R_s of the derivative-based cells. All the cells based on the pentacene derivatives showed a significant increase of V_{oc}, compared to that of pure pentacene (0.24 V), ranging from 0.57 V for TP-5, 0.69 for EtTP-5, and 0.90 V for TIPS. The open circuit voltage for the TIPS/C_{60} cell is among the highest reported to date for small molecule-based organic photovoltaics [2,25]. Examples of electron donors yielding values of V_{oc} approaching 1 V in cells with C_{60} include 4,4-bis[*N*-1-naphthyl-*N*-phenyl-amino]biphenyl (α-NPD) [26] and subphthalocyanines [27]. We note that the photocurrent density and dark current density are similar above V_{oc} for all devices, suggesting that there is no significant photoenhanced conductivity. J_{sc} is proportional to the illumination intensity, indicating that exciton-exciton annhilation was not a significant loss mechanism in these cells.

Fig. 5 shows a qualitative correlation between V_{oc} and the oxidation potential of pentacene and the derivatives. TIPS has the highest oxidation potential of 0.39 V while pentacene the lowest of 0.10 V, measured relative to a ferrocene standard. Gas phase photoemission measurements

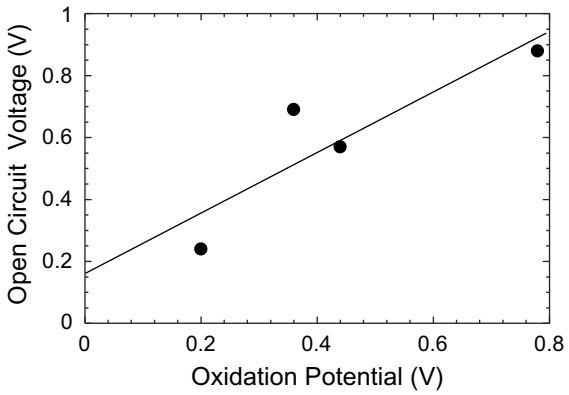

Fig. 5. Variation of V_{oc} with the oxidation potential of the electron donor molecules.

show a similar trend with the vertical ionization energy being higher for TIPS (6.38 eV) than for TP-5 (6.20 eV) or EtTP-5 (6.01 eV) [28]. It is worth noting that there is not a 1:1 correspondence between V_{oc} and the oxidation potentials of the various pentacene derivatives. This can be partly attributed to the effect of polarization energy in the solid state, which can be as high as a few tenths of eV. The injection conditions at the interface between PEDOT:PSS and electron donor should also be considered. V_{oc} depends on the amount of injected holes according to Eq. (2), which is a rearrangement of the Shockley equation [2]

$$V_{oc} = \frac{nk_BT}{q} \ln\left(1 + \frac{I_{ph} - V_{oc}/R_{sh}}{I_0}\right) \quad (2)$$

where k_B is the Boltzmann constant, q the electron charge, T the temperature in Kelvin, I_{ph} the photocurrent and I_0 is the reverse saturation current. Increased hole injection from the anode would result in a larger dark current opposing the photocurrent. The shunt resistance of the pentacene derivative cells, determined by a linear fit to the reverse bias dark current, exceeded $10^5\ \Omega\ cm^2$ and thus the leakage current will be of order $\mu A/cm^2$, two orders of magnitude lower than the photocurrent. Hence, the shunt resistance only plays a minor role in determining the open circuit voltage of these cells.

Fig. 6a compares the IPCE spectra of the various cells. Pentacene cells show the highest efficiency of 72% at 660 nm suggesting that exciton diffusion and charge transfer are efficient processes. The strong contribution of unsubstituted pentacene is consistent with the long exciton diffusion length ($\geqslant$50 nm) that has been reported [6]. On the other hand, all pentacene derivatives have much lower efficiencies, 16% or less within the longer-wavelength absorption bands, where excitons are generated in the pentacene layers. The IPCE spectra of the pentacene derivative cells follow the absorption spectrum of C_{60} with some additional contributions in the red. It is quite surprising that there is no evidence of the strong absorption in the blue for TP-5 and EtTP-5 in the IPCE spectra of devices based on these derivatives. These spectra demonstrate that the primary charge generation pathway is absorption by C_{60} followed by charge transfer at the organic heterojunction. Fig. 6b compares the IPCE spectrum of the TP-5 device with the calculated absorption of a bi-layer film consisting of 40 nm of C_{60} and 40 nm of TP-5. The two spectra diverge where TP-5 absorbs strongly between 400 and 500 nm. The sharp absorption peak of TP-5 permits a rough estimation of the diffusion length by taking the absorbance as a function of the depth profile of the bi-layer structure (neglecting thin film interference effects). A very short exciton diffusion length should result in a dip in the IPCE spectrum at λ = 470 nm, as the TP-5 layer will filter light from the heterojunction. Likewise, an exciton diffusion length comparable to the film thickness, should result in a peak at this wavelength. A good fit to the IPCE spectrum between 400 and 500 nm could be obtained for an exciton diffusion length of 18–20 nm (Fig. 6b). We propose that the weaker intermolecular coupling in the derivative films inhibits exciton diffusion, in which case thicker layers increase the series resistance, but do not yield additional photocurrent.

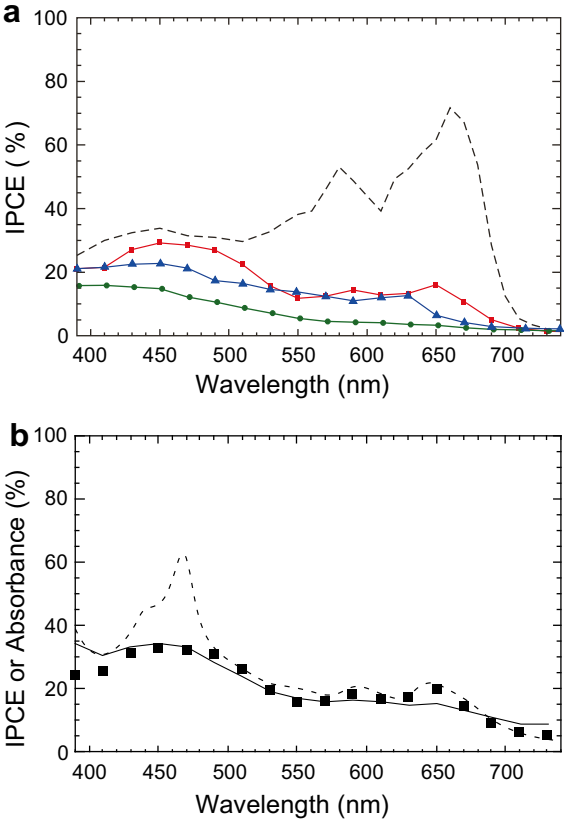

Fig. 6. (a) IPCE spectra of solar cells based on pentacene (black line) and its derivatives [TIPS (green, circles), TP-5 (red, squares), and EtTP-5 (blue, triangles)]. (b) Comparison of the IPCE spectrum of a TP-5 based cell (symbols) to the calculated absorbance of a TP-5/C_{60} bilayer film (dashed line) and a simulated IPCE spectrum taking into account the exciton diffusion length of TP-5 (solid line). (For interpretation of the references to colour in this figure legend, the reader is referred to the web version of this article.)

This hypothesis was confirmed by examining the effect of the thickness of the pentacene derivative layer on cell performance. The thicknesses of the C_{60} and BCP layers were fixed at 40 nm and 10 nm, respectively. Table 2 compares V_{oc}, J_{sc}, and η for TP-5 and EtTP-5 based pentacene/C_{60} cells with different TP-5 and EtTP-5 layer thicknesses. V_{oc} is unaffected by the thickness of the EtTP-5 layer, indicating that the offset between the HOMO of EtTP-5 and LUMO of C_{60} plays a determining role in this system. The

Table 2
Dependence of the photovoltaic cell parameters of TP-5 and EtTP-5 based solar cells on the thickness of the pentacene derivative layer

Electron donor (thickness)	V_{oc} (V)	J_{sc} (mA/cm^2)	*ff*	η (%)
TP-5 (12 nm)	0.45	1.81	0.41	0.33
TP-5 (23 nm)	0.56	2.46	0.41	0.56
TP-5 (38 nm)	0.57	2.32	0.37	0.50
EtTP-5 (12 nm)	0.72	2.40	0.43	0.74
EtTP-5 (23 nm)	0.72	1.97	0.40	0.57
EtTP-5 (38 nm)	0.69	1.68	0.29	0.34

All devices have 40 nm thick C_{60} and 10 nm thick BCP layers.

fill factor and current density, however, decrease monotonically with cell thickness. Increased absorption by EtTP-5 is more than offset by poor carrier extraction owing to the particularly low hole mobility of this material. Thus, the primary role played by EtTP-5 is to sensitize charge photogeneration at the organic heterojunction. The maximum efficiency ($\eta = 0.74\%$) therefore occurs for the thinnest (13 nm) EtTP-5 layer. For TP-5, the maximum efficiency is ($\eta = 0.56\%$) for a thickness of 24 nm, in good agreement with the estimated diffusion length. For the thinnest cell, efficiency is limited by light absorption of TP-5 and as its thickness increases, the series resistance limits the cell efficiency. These maximum efficiencies are slightly below that of the reference pentacene cell (0.82%).

4. Conclusions

In summary, we have demonstrated organic solar cells based on a series of pentacene derivatives functionalized by triisopropylsilylethynyl and dioxolane substitution. High open circuit voltages and reasonable power conversion efficiencies were obtained for solar cells based on these materials. V_{oc} of these cells correlates nicely with the oxidation potential of the donor pentacene derivative. The power conversion efficiency of these cells reached 0.74% and was limited by the series resistance and photocurrent generation efficiency. We attribute these effects to the amorphous nature of pentacene derivative films prepared by sublimation onto unheated substrates. As improved charge transport within the pentacene derivative layer has been demonstrated [21,23], significant improvements in efficiency may be expected with optimization of both the deposition conditions and the device architecture.

Acknowledgements

The authors would like to thank Dr. Mason Wolak for measuring the absorption spectra of TIPS and Olga Lobanova and Dennis Lichtenberger for providing preliminary gas phase photoemission data. This work was supported by the Office of Naval Research.

References

[1] C.W. Tang, Appl. Phys. Lett. 48 (1986) 183–185.
[2] P. Peumans, A. Yakimov, S.R. Forrest, J. Appl. Phys. 93 (2003) 3693–3723.
[3] C.-W. Chu, Y. Shao, V. Shrotriya, Y. Yang, Appl. Phys. Lett. 86 (2005) 243506.
[4] Y. Shao, S. Sista, C.W. Chu, D. Sievers, Y. Yang, Appl. Phys. Lett. 90 (2007) 103501.
[5] A.C. Mayer, M.T. Lloyd, D.J. Herman, T.G. Kasen, G.G. Malliaras, Appl. Phys. Lett. 85 (2004) 6272–6274.
[6] S. Yoo, B. Domercq, B. Kippelen, Appl. Phys. Lett. 85 (2004) 5427–5429.
[7] A.K. Pandey, J.-M. Nunzi, Appl. Phys. Lett. 89 (2006) 213506.
[8] Y. Kinoshita, T. Hasobe, H. Murata, Appl. Phys. Lett. 91 (2007) 083518.
[9] J. Yang, T.Q. Nguyen, Org. Electron. 8 (2007) 566–5674.
[10] A. Maliakal, K. Raghavachari, H. Katz, E. Chandross, T. Siegrist, Chem. Mater. 16 (2004) 4980–4986.
[11] H. Klauk, M. Halik, U. Zschieschang, G. Schmid, W. Radlik, J. Appl. Phys. 92 (2002) 5259–5263.
[12] N.J. Watkins, L. Yan, Y.L. Gao, Appl. Phys. Lett. 80 (2002) 4384–4386.
[13] J.E. Anthony, J.S. Brooks, D.L. Eaton, S.R. Parkin, J. Am. Chem. Soc. 123 (2001) 9482–9483.
[14] C.D. Sheraw, T.N. Jackson, D.L. Eaton, J.E. Anthony, Adv. Mater. 15 (2003) 2009–2011.
[15] M.M. Payne, J.H. Delcamp, S.R. Parkin, J.E. Anthony, Org. Lett. 6 (2004) 1609–1612.
[16] M.A. Wolak, B.B. Jang, L.C. Palilis, Z.H. Kafafi, J. Phys. Chem. B 108 (2004) 5492–5499.
[17] L.C. Palilis, J.S. Melinger, M.A. Wolak, Z.H. Kafafi, J. Phys. Chem. B 109 (2005) 5456–5463.
[18] M.A. Wolak, J. Delcamp, C.A. Landis, P.A. Lane, J. Anthony, Z.H. Kafafi, Adv. Funct. Mater. 16 (2006) 1943–1949.
[19] M.T. Lloyd, A.C. Mayer, A.S. Tayi, A.M. Bowen, T.G. Kasen, D.J. Herman, D.A. Mourey, J.E. Anthony, G.G. Malliaras, Org. Electron. 7 (2006) 243–248.
[20] J.E. Anthony, J. Gierschner, C.A. Landis, S.R. Parkin, J.B. Sherman, R.C. Bakus, Chem. Commun. 45 (2007) 4746–4748.
[21] O. Ostroverkhova, S. Shcherbyna, D.G. Cooke, R.F. Egerton, F.A. Hegmann, R. Tykwinski, S.R. Parkin, J.E. Anthony, J. Appl. Phys. 98 (2005) 033701.
[22] J.G. Park, R. Vasic, J.S. Brooks, J.E. Anthony, J. Appl. Phys. 100 (2006) 044511.
[23] S.K. Park, T.N. Jackson, J.E. Anthony, D.A. Mourey, Appl. Phys. Lett. 91 (2007) 063514.
[24] I.G. Hill, A. Kahn, J. Appl. Phys. 86 (1999) 2116–2122.
[25] B.P. Rand, J. genoe, P. Heremans, J. Poortmans, Progr. Photovolt. 15 (2007) 659.
[26] G.P. Kushto, W.H. Kim, Z.H. Kafafi, Appl. Phys. Lett. 86 (2005) 093502.
[27] K.L. Mutoloo, E.I. Mayo, B.P. Rand, S.R. Forrest, M.E. Thompson, J. Am. Chem. Soc. 128 (2006) 8108–8109.
[28] O. Lobanova, private communication.